HHS Public Access

Author manuscript

Clin Cancer Res. Author manuscript; available in PMC 2019 August 15.

Published in final edited form as:

Clin Cancer Res. 2019 February 15; 25(4): 1343–1357. doi:10.1158/1078-0432.CCR-18-0372.

A combination CDK4/6 and IGF1R inhibitor strategy for Ewing sarcoma

Lillian M. Guenther[1], **Neekesh V. Dharia**[1,2], **Linda Ross**[1], **Amy Conway**[1], **Amanda L. Robichaud**[1], **Jerrel L. Catlett II**[1], **Caroline S. Wechsler**[1], **Elizabeth S. Frank**[1,2], **Amy Goodale**[2], **Alanna J. Church**[3], **Yuen-Yi Tseng**[2], **Rajarshi Guha**[4], **Crystal G. McKnight**[4], **Katherine A. Janeway**[1], **Jesse S. Boehm**[2], **Jaume Mora**[5], **Mindy I. Davis**[4], **Gabriela Alexe**[1,2,6], **Federica Piccioni**[2], and **Kimberly Stegmaier**[1,2]

[1]Department of Pediatric Oncology, Dana-Farber Cancer Institute and Boston Children's Hospital, Boston, Massachusetts [2]Broad Institute, Cambridge, Massachusetts [3]Department of Pathology, Boston Children's Hospital, Boston, Massachusetts [4]Division of Preclinical Innovation, National Center for Advancing Translational Sciences, National Institutes of Health, Rockville, Maryland [5]Department of Pediatric Oncology and Hematology, Hospital Sant Joan de Déu, Barcelona 08950, Spain [6]Bioinformatics Graduate Program, Boston University, Boston, Massachusetts

Abstract

Introduction: Novel targeted therapeutics have transformed the care of subsets of patients with cancer. In pediatric malignancies, however, with simple tumor genomes and infrequent targetable mutations, there have been few new FDA-approved targeted drugs. The cyclin-dependent kinase (CDK)4/6 pathway recently emerged as a dependency in Ewing sarcoma. Given the heightened efficacy of this class with targeted drug combinations in other cancers, as well as the propensity of resistance to emerge with single agents, we aimed to identify genes mediating resistance to CDK4/6 inhibitors and biologically relevant combinations for use in Ewing.

Experimental Design: We performed a genome-scale open reading frame (ORF) screen in two Ewing cell lines sensitive to CDK4/6 inhibitors to identify genes conferring resistance. Concurrently, we established resistance to a CDK4/6 inhibitor in a Ewing cell line.

Results: The ORF screen revealed *IGF1R* as a gene whose overexpression promoted drug escape. We also found elevated levels of phospho-IGF1R in our resistant Ewing cell line, supporting the relevance of IGF1R signaling to acquired resistance. In a small-molecule screen, an IGF1R inhibitor scored as synergistic with CDK4/6 inhibitor treatment. The combination of CDK4/6 and IGF1R inhibitors were synergistic *in vitro* and active in mouse models. Mechanistically, this combination more profoundly repressed cell cycle and PI3K/mTOR signaling than either single drug perturbation.

Corresponding Author: Kimberly Stegmaier, MD, Dana-Farber Cancer Institute, 450 Brookline Avenue, Boston, Massachusetts 02215, Tel: 617-632-4438 Fax:617-632-4850, Kimberly_Stegmaier@dfci.harvard.edu.

Conflict of Interest Disclosure Statement: K. Stegmaier participates in the DFCI/Novartis Drug Discovery Program which includes grant support and previously included consulting and has consulted for Rigel Pharmaceuticals on a topic unrelated to this manuscript.

Conclusions: Taken together, these results suggest that IGF1R activation is an escape mechanism to CDK4/6 inhibitors in Ewing sarcoma and that dual targeting of CDK4/6 and IGF1R provides a candidate synergistic combination for clinical application in this disease.

INTRODUCTION

The characterization of the landscape of somatic mutations in cancer through massively parallel sequencing (1) has led to the investigation and subsequent FDA-approval of several new classes of drugs that capitalize on molecular alterations inherent to cancer cells. As effective targeted therapies have emerged, these have been combined with traditional chemotherapies in select malignancies in order to achieve more prolonged disease response and lessen treatment-related morbidity. In some select instances, such as in the treatment of chronic myelogenous leukemia (CML) and acute promyelocytic leukemia (APML), targeted therapies have even replaced standard cytotoxic medications.(2)

A drug class that has gained traction in multiple adult malignancies is inhibitors against cyclin-dependent kinase (CDK)4/6. CDK4/6 inhibitors are FDA-approved for the up-front treatment of hormone receptor positive (HR+), HER2 negative breast cancer. In this disease, CDK4/6 overexpression, as well as *CCND1* amplification, are frequent driver events and were found to underlie resistance to estrogen receptor (ER) antagonists, a backbone of HR+ breast cancer treatment.(3) The combination of CDK4/6 inhibitors with ER antagonists was active in multiple clinical trials, dramatically improving event-free survival (EFS) compared to ER antagonist treatment alone, and this combination has become standard of care in the up-front setting for these patients.(4, 5) CDK4/6 inhibitors have subsequently been found to have efficacy for patients with liposarcoma, who frequently have *CDK4* amplifications, as well as for patients with *KRAS* mutant non-small cell lung cancer (NSCLC).(6, 7)

In pediatric malignancies, the search for useful targeted therapies has been more challenging given their relatively quiet genomes, with few recurrent targetable somatic mutations. We became interested in CDK4/6 inhibitors in Ewing sarcoma, an aggressive pediatric solid tumor, after identifying *CDK4* as a Ewing-selective dependency gene. *CDK4* scored at the intersection of Ewing sarcoma super-enhancer profiling, genome-scale shRNA screening, and chemical library screening, and CDK4/6 inhibitors showed promising activity *in vitro* and *in vivo* in Ewing sarcoma models.(8) Ewing sarcoma is a poorly differentiated small round blue cell tumor and is the second most common malignant bone tumor affecting children and young adults. Despite advances in survival with the use of multimodality treatment strategies, cure rates in children with localized disease remain stagnant at 70%, and children diagnosed with metastatic disease have a dismal five-year survival of less than 30%.(9) New treatment strategies are urgently needed to improve outcomes in this disease. Despite our own and others' investigation of CDK4/6 inhibitors in preclinical models of Ewing sarcoma,(8, 10, 11) CDK4/6 inhibitors have yet to be tested in clinical trials in children with this disease. However, there is an expanding interest in pediatric applications. In addition to Ewing sarcoma data, there is pre-clinical data supporting the activity of CDK4/6 inhibitors in rhabdomyosarcoma, neuroblastoma, as well as T-ALL. Moreover, a Phase 1 study has demonstrated tolerability of this compound class in children, and a subset

of patients with neuroblastoma and malignant rhabdoid tumors achieved stable disease with CDK4/6 inhibitor treatment. (12–15)

CDK4/6 inhibitors typically induce cell cycle arrest rather than cell death. Therefore, as observed in the treatment of patients with breast cancer, CDK4/6 inhibitors are unlikely to have long-term efficacy as monotherapy in most aggressive malignancies, including Ewing sarcoma. In addition, single agent cancer therapy generally does not lead to durable remissions given the inevitable emergence of resistant clones. In the case of CDK4/6 inhibitors, acquired resistance has been observed both in pre-clinical models (16, 17) and in patient samples (18) through mechanisms such as inactivating mutations in *RB1*, a tumor suppressor whose function is required for the activity of CDK4/6 inhibitors. In addition, upregulation of other D-type cyclins and utilization of non-canonical cell cycle entry have been observed as a mechanism to circumvent drug activity in both breast cancer and leukemia models.(16, 19)

Strategies to anticipate and overcome resistance are therefore critical to the development of effective small-molecule therapeutic combinations. To address this challenge, we deployed a genome-scale open reading frame (ORF) screen in combination with CDK4/6 inhibitors, with the goals of identifying genes involved in resistance to CDK4/6 inhibitors in Ewing sarcoma and informing secondary targets for combination therapies. In parallel, we also performed a small molecule screen to more directly identify molecules that are synergistic with CDK4/6 inhibitors in Ewing sarcoma. IGF1R scored at the intersection of these two screens. Here, we report IGF1R activation as a mediator of resistance to CDK4/6 inhibitors and the dual targeting of IGF1R and CDK4/6 as synergistic *in vitro* and *in vivo* in Ewing sarcoma, supporting a combination of these drugs for the treatment of this disease.

MATERIALS AND METHODS

Established cell lines and chemicals

All cell lines were cultured at 37°C in a humidified atmosphere containing 5% CO2. A673, SKNEP1, SKNMC, and the SKPNDW lines were grown in Dulbecco's Modified Eagle's Media (Life Technologies) supplemented with 10% fetal bovine serum (FBS) (Sigma-Aldrich). A673 cells were supplemented with 1 mmol/L of sodium pyruvate (Life Technologies). The CADOES1 and TC32 lines were cultured in RPMI1640 (Sigma-Aldrich) with 15% and 10% FBS, respectively. All cells were grown in the presence of 10 units/mL of penicillin, 10 μg/mL streptomycin and 30 μg/mL of L-Glutamine, PSQ (Thermo Fisher Scientific). Whole exome sequencing, RNA sequencing and STR genotyping of all Ewing sarcoma cell lines used in these studies and validated cell line identity.(20) Cell lines were regularly tested for *Mycoplasma* by PCR (Sigma Aldrich). All cell lines were passaged between 4–12 weeks between thawing and use in the described experiments. All cell lines were a kind gift from Todd Golub (Broad Institute, Cambridge, MA), Nathanael Gray (Dana-Farber Cancer Institute, Boston, MA). Ewing sarcoma cell lines were treated with the CDK4/6 inhibitor ribociclib and the IGF1R inhibitor AEW541 kindly provided by Novartis Oncology. Palbociclib (Cat. No S1116), linsitinib (Cat. No S1091), and GDC0941 (Cat. No S1065) were obtained from Selleck Chemicals. THZ1 was a kind gift from Nathanael Gray.

Lentivirus production and transduction

Lentivirus was produced by transfecting HEK-293T cells with the appropriate lentiCRISPRv2 sgRNA vector, a gift from Feng Zhang (Addgene plasmid #52961),(21) and the packaging plasmids pCMV8.9 and pCMV-VSVG, using Xtremegene 9 per the manufacturer's instructions (Thermo-Scientific). CRISPR sgRNAs sequences for *IGF1R* were obtained for lentiviral transduction, and Ewing sarcoma cells were incubated with 2 mL of virus and 8 μg/mL of polybrene (Sigma-Aldrich). Cells were selected in puromycin (Sigma-Aldrich) 48 hours post-transduction. Six days post-selection, cells were harvested for protein and viability assays in drug treatment. CRISPR guide sequences against *CDK4* were from the Achilles Project Avana library at the Broad Institute. sgRNAs against *IGF1R* were designed using the Broad Institute sgRNA designer tool (http://www.broadinstitute.org/rnai/public/analysis-tools/sgrna-design-v1). NT guides were designed to initiate double-stranded breaks in non-coding regions of the genome. sgRNA sequences were as follows: NT_1:GTAGCGAACGTGTCCGGCGT; NT_2:GACCGGAACGATCTCGCGTA; CDK4_1:AAGAGTGTGAGAGTCCCCAA; CDK4_2:CCAGTGGCTGAAATTGGTGT; CDK4_3:GGCCTTGTACACTGTCCCAT; CDK4_4:GTCTACATGCTCAAACACCA; IGF1R_2:TATCCACAGCTGCAACCACG; IGF1R_3:GTACTTGCTGCTGTTCCGAG; IGF1R_4:TCGGGCAAGGACCTTCACAA

Determination of cell viability and synergy studies

Cells were seeded onto 384-well tissue culture treated plates at a density of 25,000 cells/ml. 96-well drug plates were created such that each plate contained one compound serially diluted 1:2 at dose range specified with DMSO controls and compounds were transferred robotically. After treatment with a single compound (single agent IC_{50}) or combination of compounds (synergy studies) at serial two-fold dilutions, plated cells were analyzed for cell viability at the time points specified (zero to five days) using the Cell-TiterGlo luminescence assay (Promega) per the manufacturer's instructions. Luminescence was read on a Fluostar Omega Reader (BMG Labtech). IC_{50} values were calculated from ATP luminescence measurements using log-transformed, normalized data in GraphPad Prism 5.0 (GraphPad Software, Inc.).

Western immunoblotting

Cells were lysed in Cell Signaling Lysis Buffer (Cell Signaling Technology) supplemented with Complete, EDTA free Protease Inhibitor Cocktail (Roche Diagnostics) and Phos-STOP Phosphatase Inhibitor (Roche Diagnostics). Protein concentrations were determined by the Bradford protein assay. Protein samples were separated by SDS-PAGE and transferred to PVDF membranes. Membranes were incubated with primary antibodies directed against CDK4 (Cell Signaling Technology Cat. No. 12790), IGF1R beta (Cell Signaling Technology Cat. No. 3018), p-Tyr1135-IGF1R beta (Cell Signaling Technology Cat. No. 3918), RB (Cell Signaling Technology Cat. No. 9309), p-Ser780-Rb (Cell Signaling Technology Cat. No.9307), p-Ser807/811-Rb (Cell Signaling Technology Cat. No. 9308), AKT (Cell Signaling Technology Cat. No. 9272), p-Ser473-AKT (Cell Signaling Technology Cat. No. 9271), S6-Ribosomal Protein (Cell Signaling Technology Cat. No. 2217), p-Ser240/244-S6 Ribosomal Protein (Cell Signaling Technology 2215), p-Ser235/236-S6 Ribomal Protein

(Cell Signaling Technology Cat. No. 2211), 4E-BP1 (Cell Signaling Technology Cat. No. 9644), p-Thr37/46–4E-BP1 (Cell Signaling Technology Cat. No. 2855), PARP (Cell Signaling Technology Cat. No. 9542), total caspase 3 (Cell Signaling Technology Cat. No. 9662), cleaved caspase 3 (Cell Signaling Technology Cat. No. 9664), GAPDH (Santa Cruz Biotechnology Cat. No. sc-137179), tubulin (Sigma Cat. No. T6199), vinculin (Abcam Cat. No 18058), and β-Actin (Cell Signaling Technology Cat. No. 3700). Horseradish peroxidase (HRP) conjugated secondary antibodies were used. Blots were visualized by enhanced chemi-luminescence (ThermoFisher Scientific).

Serial cell counting

TC32 and SKNEP1 Ewing sarcoma cells were grown in 6-well plates at a starting density of 100–400k cells per well and, 24 hours after plating, were treated with 1 μM AEW541, 1 μM ribociclib, a combination of 1 μM AEW541 and 1 μM ribociclib, or DMSO controls. At serial time points cells were trysinized, quenched, and counted using the Countess™ II automated cell counter (Invitrogen) to assess number of viable cells present. Media with drug(s) or DMSO was changed every four days.

Cell Cycle Analysis and Cell Death Assays

The effect of AEW541, ribociclib, or combination treatment on Ewing sarcoma cell cycling was measured at 120 hours post-treatment. Cells were harvested, washed and fixed in ethanol and then re-suspended in 40 μg/mL propidium iodide (Sigma-Aldrich) and 100 μg/mL of RNase A (Qiagen). Samples were analyzed on a FACSCanto II analyzer. Ewing sarcoma cells lines were assessed for cell death after single or combined small-molecule treatment at 120 hours post-treatment. Cell death was assessed using flow cytometric analysis of annexin V and propidium iodide staining according to the manufacturer's instructions (eBioscience). Data analysis was completed using Flowjo 7.6 software (Treestar).

Beta-Galactosidase Senescence Staining

The effect of AEW541, ribociclib, or combination treatment on Ewing sarcoma cell senescence was measured at 120 hours post-treatment using senescence-associated β-galactosidase activity (SA-β-gal). TC32 cells infected with a previously reported TRIPZ inducible small hairpin against EWS/FLI(22) were used as a positive control for senescence 120 hours after doxycycline induction,(23) as were senescent mouse embryonic fibroblasts (MEF). Fixing and staining was completed and cells were incubated overnight according to manufacturer's instructions (Cell Signaling).

In vivo tumor models

A PDX mouse model of Ewing sarcoma with a type I EWS/FLI fusion was established from a tumor resected from the fibula of a 12-year-old patient at diagnosis (HSJD-ES-002). HSJD-ES-002 was established in athymic nude mice (Harlan, Barcelona, Spain) as previously described (24). Informed consent for the use of clinical data and biological material was obtained and all studies were approved by the ethics review committee at the Sant Joan de Déu Hospital in Barcelona. All dosing studies were performed at the Dana-

Farber Cancer Institute, and all animal protocols were approved by the Dana-Farber Cancer Institute Animal Care and Use Committee (IACUC). Nude mice were maintained according to institutional guidelines.

AEW541 and ribociclib combination studies—Three million A673 cells were subcutaneously implanted into the right flanks of 7–8 week old nude female mice. For PDX studies, 1 mm^3 viably frozen tumor chunks were dipped in matrigel and implanted into the right flanks via minor surgery. When tumors measured 100–150 mm^3, mice were divided into four groups: vehicle control, AEW541, ribociclib, and AEW541 and ribociclib in combination. AEW541 was administered by oral gavage BID at 50 mg/kg, and ribociclib was administer by oral gavage daily at 75 mg/kg. Tumors were measured twice per week and mice were followed for survival. Statistical significance was determined by log-rank test for survival curves.

Quantification and statistical analyses

GraphPad PRISM 7, R 3.2.3 and Python 2.7.2 software packages were used to perform the statistical analyses. Statistical tests used are specified in the Figure legends. Errors bars represent standard deviation, unless otherwise stated. The threshold for statistical significance is $P < 0.05$, unless otherwise specified.

All studies with human experimentation (low-passage cell lines, PDX models) were conducted in accordance with the Declaration of Helsinki.

Please see supplemental methods for additional information on experimental techniques.

RESULTS

CDK4 is a top target nominated by multiple genomic screens in Ewing sarcoma.

Recent massively parallel sequencing efforts have revealed that many pediatric tumors, including Ewing sarcoma, frequently have very quiet genomes, with few targetable alterations.(1, 20, 25, 26) Previously, we reported that CDK4 is a top Ewing sarcoma dependency by shRNA screening compared to hundreds of other cancer cell lines screened. (8) We have now completed and analyzed a genome-scale CRISPR-Cas9 screen in 476 cancer cell lines that again identified CDK4 as a top Ewing dependency compared to the other cell lines screened (Figure 1A; Supplemental Figure 1; Supplemental Table 1). We validated this finding by CRISPR knockout of *CDK4* in the Ewing sarcoma cell line A673 and demonstrated marked impairment in cell growth (Figure 1B-C).

CDK4/6 inhibitors have efficacy in HR+ breast cancer and have been FDA-approved for up-front therapy in combination with ER antagonists in this disease. We thus compared the degree of dependency of Ewing sarcoma cell lines on CDK4 to that of HR+ breast cancer cell lines included in the Achilles shRNA screen.(27) This effort included 9 Ewing sarcoma cell lines and 12 HR+ breast cancer cell lines. Ewing sarcoma and HR+ breast cancer cell lines were equally dependent on CDK4 (Figure 1D). Therefore, with strong evidence of Ewing sarcoma dependency on CDK4, we further investigated the application of CDK4/6 inhibitors in this disease.

An ORF screen identifies IGF1R overexpression as a resistance mechanism to CDK4/6 inhibitors in Ewing sarcoma

As has been extensively reported in pre-clinical breast cancer studies, CDK4/6 inhibitors are generally ineffective as single agents, where acquired resistance is observed via mechanisms such as the loss of *RB1*, amplification or upregulation of other CDKs leading to alternative cell cycle entry, or activation of growth signaling pathways, such as PI3K/AKT.(16, 28, 29) We sought to identify potential resistance mechanisms to CDK4/6 inhibitors in Ewing sarcoma, reasoning that the discovery of targetable genes rendering resistance to CDK4/6 inhibitors may inform efficacious drug combinations. We performed a barcoded, genome-scale, lentiviral-delivered ORF screen in Ewing sarcoma cells that included 17,255 clones overexpressing 12,952 proteins with at least 99% nucleotide and protein match. The screen was performed in two Ewing sarcoma cell lines, SKNEP1 and TC32, which were chosen given their sensitivity to CDK4/6 inhibitors. Transduced, pooled and selected cells were grown in the presence or absence of IC_{90} concentrations of the CDK4/6 inhibitors palbociclib and ribociclib for 19 days. At the end of this period, when increased growth rates of drug-treated ORF-library infected cells were observed, indicative of treatment resistance, genomic DNA was collected and sequenced for identification and quantification of barcodes. A core list of genes whose overexpression rendered resistance to each CDK4/6 inhibitor was generated by examining z-scores calculated on barcode reads and by normalizing these to an early time point (ETP). Genes scoring at the intersection of both cell lines and with both inhibitors were prioritized as core ORF hits. Two *IGF1R* ORF clones scored as rendering resistance to CDK4/6 inhibitors in both lines. A third *IGF1R* ORF also scored in SKNEP1 cells (Figure 1E). Multiple other ORF clones signaling downstream of *IGF1R,* such as *PIK3CA,* also scored (see Supplemental Table 2), heightening our interest in targeting this pathway.

We next validated this finding using a flow cytometry-based *in vitro* competition assay. We infected TC32 Ewing sarcoma cells with two *IGF1R* ORF constructs that matched to the transcript variant 1 of *IGF1R* with one base pair difference (silent): IGF1R #1 and IGF1R #2. After confirmation of overexpression of IGF1R by immunoblotting (Figure 1F), we combined each *IGF1R* ORF-infected cell population with TC32 cells infected with a GFP control ORF in a 1:1 ratio. We then grew and passaged these cells under continuous treatment with 1 μM ribociclib or 500 nM palbociclib, IC_{75} concentrations for these cell lines, or matched DMSO controls. After 14 days of treatment, flow cytometry was performed to measure the percentage of GFP-positive control versus *IGF1R* overexpressing cells. TC32 cells overexpressing both of the *IGF1R* ORFs significantly outgrew GFP control cells during treatment with ribociclib or palbociclib, but were not at a growth advantage in the DMSO controls, suggesting that *IGF1R* overexpression rendered resistance to CDK4/6 inhibitors (Figure 1G).

IGF1R drives acquired resistance to CDK4/6 inhibitors in Ewing sarcoma cell lines

In order to assess the relevance of IGF1R upregulation in acquired resistance to CDK4/6 inhibitors in Ewing sarcoma, we developed a resistant cell line by chronically exposing SKNEP1 cells in culture media to increasing concentrations of ribociclib. These ribociclib-resistant cells were also resistant to palbociclib, suggesting a class effect (Figure 2A). With

drug removal for up to 8 weeks and then re-exposure, we observed persistent drug resistance, suggesting an irreversible resistance phenomenon. SKNEP1 resistant (SKNEP1-R) cells proliferated at a faster rate than parental SKNEP1, as measured by an ATP-based assay, suggesting an alteration of growth signaling (Figure 2B). Importantly, as acquired *RB1* mutations are observed in resistance to CDK4/6 inhibitors (16, 18, 30), we confirmed that phospho and total Rb expression were still present by immunoblotting in SKNEP1-R cells. We did, however, observe an attenuated reduction of phospho-Rb levels upon treatment with escalating concentrations of ribociclib in the SKNEP1-R cells, suggesting impaired target inhibition in this resistance model (Figure 2C). Interestingly, we found that SKNEP1-R cells expressed higher levels of phospho-IGF1R by immunoblotting compared with parental SKNEP1 cells, suggesting activation of this pathway in acquired resistance to CDK4/6 inhibitors in Ewing sarcoma (Figure 2D).

To additionally characterize our resistant cells, as an alternative cell cycle entry is a known escape mechanism of CDK4/6 inhibitors, we next examined levels of CDK4 and CDK6, as well as cyclin D1, D3, and the G2/M transition-related proteins CDK2, cyclin B1, cyclin E2, and Aurora B by western immunoblotting in our SKNEP1-R cells compared with SKNEP1 cells. We found that CDK6, which also scored as a mechanism of resistance to CDK4/6 inhibitors in our ORF screen, had upregulated expression in the resistant line. In addition, cyclin B1, and cyclin E2 were upregulated in the resistant cells, suggestive of cell cycle escape in the context of CDK4/6 inhibitor resistance (Figure 2E). Importantly, whole exome sequencing of the SKNEP1-R line revealed no mutations in *RB1* or *IGF1R*, and no copy number changes in any of the upregulated cyclin/CDK proteins compared with parental SKNEP1 (Supplemental Figure 1C, Supplemental Table 3). Additionally, there were no copy number changes in the genes encoding these proteins in any of the Ewing sarcoma cell lines in our CRISPR/Cas9 screen (Supplemental Figure 1D).

In order to assess the role of activated IGF1R in driving resistance to CDK4/6 inhibition in SKNEP1-R cells, we performed CRISPR knockout (KO) of *IGF1R*. After validating KO by immunoblotting (Figure 2F), we performed ATP-based viability assays after exposure to the CDK4/6 inhibitor ribociclib for 5 days. There was a significant shift in the IC_{50} of the *IGF1R* CRISPR KO SKNEP1-R cells, compared to non-targeting control expressing SKNEP1-R cells, when exposed to a range of 39 nM to 10 μM ribociclib for five days, demonstrating partial rescue of sensitivity to CDK4/6 inhibitors when *IGF1R* levels are diminished in these cells (Figure 2G). When we examined growth rates of *IGF1R* KO SKNEP1-R cells compared to NT controls, we observed slowed growth, suggesting that activated IGF1R offers a survival benefit in these cells (Figure 2H).

A small-molecule screen identifies IGF1R inhibitors as synergistic with CDK4/6 inhibitors in Ewing sarcoma cells

In parallel to the ORF resistance screen, we performed a chemical library screen to identify molecules that are synergistic with CDK4/6 inhibitors in Ewing sarcoma. We focused on 22 small molecules that are of interest in Ewing sarcoma treatment (Supplemental Table 4). The Ewing sarcoma cell lines A673 and TC32 were treated for 5 days with palbociclib in combination with compounds from the library in a five-fold dilution series from 25 μM to 40

nM. Viability was assessed using an ATP-based assay. BMS-754807, a commercially available IGF1R inhibitor included in the library, scored as synergistic in both cell lines (Figure 3A). Moreover, inhibitors of signaling targets downstream of IGF1R, such as PI3K and mTOR, also scored in the screen, highlighting again the potential importance of this pathway.

Thus, with the ORF screen identifying IGF1R overexpression as rendering resistance to CDK4/6 inhibition, the relevance of IGF1R activation to acquired CDK4/6 inhibitor resistance, and the chemical screen identifying CDK4/6 inhibitors as synergistic with IGF1R inhibitors, along with the tractability of testing this combination in children with Ewing sarcoma, we sought to explore the efficacy of this compound combination. We performed short-term viability assays in a panel of established Ewing sarcoma cell lines (A673, SKNEP1, and TC32). As these well-established cell lines have been highly passaged *in vitro*, we also tested these combinations in two newly derived, minimally passaged Ewing sarcoma cell lines (CCLF_PEDS_0009_T and CCLF_PEDS_0010_T), which were confirmed to express Rb by western immunoblotting and the EWS/FLI fusion by RT-PCR (Supplemental Figure 2). Furthermore, these lines have no coding mutations in *RB1* based on whole exome sequencing. We investigated these small-molecule inhibitors in a matrix of concentrations from 20 μM down to 20 nM, with ATP content measured after five days of treatment as a surrogate for cell viability. A high degree of synergy was observed in all of the lines tested with the combination of ribociclib and AEW541, a small molecule inhibitor of IGF1R, across a wide-range of drug concentrations as measured with the Chou-Talalay combination index model (Figure 3B).(31) Given that AEW541 is a tool compound not optimized for clinical use, and to further validate whether this finding represents a class effect, we looked at ribociclib in combination with the IGF1R/Insulin Receptor (IR-1) inhibitor linsitinib, a molecule that has been tested in human clinical trials and is currently being studied in relapsed Ewing sarcoma in Europe.(32) We identified a synergistic interaction across all cell lines tested (Figure 3C). Furthermore, we tested palbociclib with AEW541 in the same cell lines, with synergy confirmed using this structurally distinct CDK4/6 inhibitor (Figure 3D).

As there is interest in the combination of PI3K inhibitors with CDK4/6 inhibitors in other malignancies, and as we found that PI3K and mTOR inhibitors also scored as synergistic with CDK4/6 inhibitors in our chemical library screen, we tested GDC0941, a combined PI3K/mTOR inhibitor, in combination with ribociclib in a subset of these cell lines and observed synergy. Additionally, we evaluated IGF1R and PI3K/mTOR in combination with CDK4/6 inhibitors in two *RB1* mutated cell lines, SKNMC and SKPNDW where, as expected, we did not observe additivity or synergy. In contrast, in SKNEP1-R, where Rb is intact, we did observe synergy, suggesting that the efficacy of CDK4/6 inhibitors can be partially restored in acquired resistance by combination therapy in the setting where heightened IGF1R signaling is present (Supplemental Figure 3).

In order to further investigate whether the drug combination was leading to increased cell death, cell cycle arrest or senescence, we first performed serial cell counting of TC32 and SKNEP cells with DMSO, AEW541, ribociclib, or the combination at synergistic concentrations over a 7-day time course. We observed cell death only in the combination

treatment group, whereas cytostasis was seen with single-agent ribociclib, and slowed growth was observed with single-agent AEW541 (Figure 4A). We next performed cell cycle analysis by propidium iodide staining with flow cytometry where we observed a G1 arrest with ribociclib treatment but an increase in the sub-G0 peak in the combination treatment consistent with cell death (Figure 4B). Cell death in this subset of cells was via an Annexin positive but apoptosis independent mechanism as combination treated cells demonstrated neither induction of cleaved PARP nor cleaved caspase 3 (Figure 4C and D). In the combination treatment, however, a subset of the cells remain viable. Using an SA-β-gal staining assay, we determined that ribociclib-treated Ewing sarcoma cells were positive for β-gal as had previously been reported with CDK4/6 inhibitor treatment in Ewing sarcoma and in other diseases (11, 12), and the viable combination treated cells were also positive, consistent with senescence (Figure 4E).

Combined treatment with IGF1R and CDK4/6 inhibitors enhances suppression of the cell cycle and PI3K/mTOR axis

Given the strong synergy of these two classes of compounds in Ewing sarcoma, we next investigated the mechanisms of IGF1R and CDK4/6 synergy in this disease utilizing a reverse phase protein array (RPPA). This antibody-based, high-throughput approach has been used extensively for studying cancer with a panel of 300 antibodies focused on tumorigenic signaling, growth factor activation and DNA damage.(33) After 48 hours of treatment with concentrations of ribociclib or palbociclib and AEW541 necessary to achieve an IC_{50} in combination based on our *in vitro* studies, TC32 Ewing sarcoma cell pellets were harvested and protein was analyzed by RPPA. As has been described in the response of breast cancer cells to CDK4/6 inhibitors,(16, 29) we found alterations of cell cycle proteins. In the combination treated cells, there was profound suppression of Cyclin B1 and CDK1. In addition, levels of phospho-Rb were further diminished in the combination compared to ribociclib alone. Cyclin D3, a catalytic partner in CDK4/6 activation, was increased with single agent ribociclib, and subsequently re-suppressed with treatment in combination, suggesting that combination treatment with an IGF1R inhibitor can prevent this potential escape mechanism to CDK4/6 inhibition (Figure 5A).

In addition to cell cycle protein alterations, there was profound suppression of the PI3K/AKT/mTOR axis. With dual inhibitor drug treatment, there was heightened effect on the suppression of phosphorylation of phospho-S6 ribosomal protein and phospho-4EBP1, with accumulation of the upstream target p70 S6 kinase and the beta subunit of PI3K in the combination treated cells compared to either single inhibitor alone. It has previously been reported in breast cancer that CDK4/6 inhibition leads to an increase in AKT phosphorylation, and PI3K inhibitors have been used in combination with CDK4/6 inhibitors with good effect in this disease setting to suppress this upregulation.(16, 34) Similarly, we observed an increase in AKT phosphorylation in cells treated with ribociclib alone. This upregulation of AKT activity was reversed with the addition of the IGF1R inhibitor AEW541 (Figure 5B). Additionally, we found that amongst our hits, a cluster of mitosis-related proteins scored in the top differentially repressed proteins with dual treatment compared to single agents (Figure 5C). These three clusters together support our findings of profound growth suppression and cell death with the combination *in vitro*

compared to either single drug treatment alone. We validated a selection of these cell cycle, PI3K/mTOR, and mitosis-related hits by western immunoblotting (Figure 5D). Subsequently, in order to evaluate the generalizability of these mechanistic findings in Ewing sarcoma, we performed inhibitor treatments in a second Ewing sarcoma cell line, SKNEP1, and western immunoblotting of the same targets, with good concordance seen between the two lines (Figure 5E).

IGF1R and CDK4/6 inhibitors are active in cell line and patient-derived xenograft (PDX) models of Ewing sarcoma

Given the strong synergy observed *in vitro*, we next tested AEW541 in combination with ribociclib in an A673 cell line xenograft, an aggressive model of Ewing sarcoma frequently used for *in vivo* studies. Nude mice were injected subcutaneously with A673 cells, and at the time of measurable tumors, were treated with vehicle, 75 mg/kg/day of ribociclib, 50 mg/kg BID of AEW541, or the combination, all dosed by oral gavage for 21 days. Tumors were measured twice per week, and the animals were followed for survival. We found significantly attenuated growth and improved survival in mice treated with the combination compared to either single agent or control treatment (Figure 6A-B). Neither weight loss nor cytopenias were observed (Supplemental Figure 4A and B). In order to validate activity in a model likely to be more faithful to patient disease, we next evaluated a PDX derived from a tumor with a type I EWS/FLI fusion resected from the fibula of a 12-year-old patient at diagnosis (HSJD-ES-002). After implantation of tumor fragments into the flanks of nude mice, we monitored mice for measurable tumors and then treated them for 28 days with doses as above in the A673 xenograft study. We observed significantly prolonged survival and mitigated tumor progression in the combination arm compared to either single agent alone (Figure 6C-D). We evaluated target inhibition in our PDX model in mice sacrificed after treatment with vehicle control, AEW541, ribociclib, or the combination at the doses above for five days. By immunohistochemistry staining for phospho Rb of three mice per treatment group, we saw a statistically significant decrease in the ribociclib and combination groups as compared to the vehicle control (Figure 6E). A trend towards decreased phospho-S6 staining in the combination arm compared to the vehicle treated arm was observed but did not reach statistical significance, likely due to the technical challenges of performing PD studies in PDX models and the small sample size (Figure 6F). There were no significant changes in necrosis measured as a percent by hematoxylin and eosin (H&E) staining (not shown). Consistent with the *in vitro* results, we did not observe differences in levels of cleaved caspase 3 staining across the groups (Figure 6G). However, we did see significantly decreased Ki67 staining in the combination group compared with controls, indicative of less cell proliferation (Figure 6H and Supplemental Figure 5).

DISCUSSION

Novel targeted drugs have revolutionized the treatment and outcome for some malignancies. Genomically quiet tumors, however, have seen few targeted therapy approvals to date. As non-mutated dependency genes are nominated by technologies such as CRISPR-Cas9 and RNAi, promising new possibilities for targeted therapies are emerging for these cancers. One such target class is CDK4/6. Drugs inhibiting these targets have altered treatment for HR+

breast cancer and have had efficacy in early phase clinical trials for a subset of patients with diseases such as liposarcoma, non-small cell lung cancer, and mantle cell lymphoma. (6, 35, 36)

CDK4/6 inhibitors have yet to be tested in patients with Ewing sarcoma; however, the level of genetic dependency on CDK4 is similar in Ewing sarcoma and HR+ breast cancer lines based on data from the Achilles shRNA screen, leading us to hypothesize that this drug class will have good clinical utility in Ewing sarcoma. Nevertheless, as combination therapy has been critical in breast cancer, it is unlikely that these drugs will be highly effective as single agents in Ewing sarcoma. In breast cancer, an early understanding of the mechanisms of resistance to endocrine therapies led to trials testing them in combination with CDK4/6 inhibitors. The success of these studies led to the approval of this combination for patients with HR+ disease. Similarly, early investigation of resistance mechanisms to BRAF inhibitors in *BRAF*-mutated melanomas led to the use of the effective combination of BRAF and MEK inhibition in upfront treatment, now standard of care.(37–39) These studies highlight the importance of developing rational targeted therapy combinations for aggressive malignancies to circumvent innate, as well as acquired resistance. As targeted therapeutics become more mainstream, the early pre-clinical investigation of resistance mechanisms is becoming a more common practice.

A specific challenge associated with CDK4/6 inhibitors is that response to single agent therapy may be attenuated by their cytostatic mechanism of action. CDK4/6 inhibitors work by impairing the phosphorylation of Rb, thus inhibiting the pro-proliferative E2F transcriptional program and halting progression from the G1 to S phase of the cell cycle.(40) CDK4/6 inhibitors, thus, typically cause cell cycle arrest rather than cell death. We have observed this in Ewing sarcoma *in vitro*, where there is predominantly cell cycle arrest with ribociclib treatment, as well as *in vivo*, where growth is attenuated; however, there is no tumor shrinkage.(8) It is therefore unlikely that these agents given as monotherapy will lead to durable disease responses in aggressive malignancies. In fact, not surprisingly, in many clinical trials testing single agent CDK4/6 inhibitors, including an early phase pediatric clinical trial, stable disease was reported as the best response.(14, 35) In addition, traditional cytotoxic agents, which are dependent on rapidly cycling cells, are often antagonistic to CDK4/6 inhibitors in *in vitro* studies, making combination strategies with these well-vetted agents challenging.(13, 41, 42) Studies to determine rational combination therapies with CDK4/6 inhibitors are, therefore, of the upmost importance for designing effective clinical trials.

As multiple therapeutic targets emerge for a specific disease from functional genomic and other screening efforts, a challenge going forward will be the identification of predictive biomarkers of response. For example, in the case of Ewing sarcoma, in addition to CDK4 and IGF1R, our group and others have identified targets such as CDK12, PARP, MDM2/MDM4 and ATR (22, 43–46). In some cases, such as for MDM2 and MDM4, a biomarker (i.e., *TP53* status) has been well validated in Ewing sarcoma and other diseases. In other cases, such as CDK12, a biomarker for response in Ewing sarcoma has yet to be determined as most of the Ewing cell lines tested were equally responsive. In the case of IGF1R inhibitors, durable responses have been observed in patients with Ewing sarcoma; however,

biomarkers of response have been elusive. For CDK4/6 inhibitors, it is well known that *RB1* loss confers intrinsic (30) and acquired (18) resistance in patients with breast cancer. Similarly, we observed intrinsic resistance in Ewing sarcoma cell lines with loss-of-function events in *RB1*. To our knowledge, however, there have been no described loss-of-function events and no recurrent copy number alterations involving *RB1* in primary Ewing sarcoma patient tumors, suggesting that this mechanism of intrinsic resistance is unlikely to be a roadblock for advancing these compounds in Ewing sarcoma. (20, 25, 26, 47) In our data, we saw no correlation between sensitivity to CDK4/6 inhibitors and other known genetic subclasses of Ewing sarcoma, including *STAG2* or *TP53* mutated. In addition, as previously reported in breast cancer (48), deletion of *CDKN2A*, the negative regulator of the cyclin D1/CDK4/6 axis, which is seen in a large subset of Ewing sarcoma, is also not correlated with differential sensitivity to CDK4/6 inhibitors in our data. Informative molecular markers of response to targeted therapies, therefore, require further study using more extensive pre-clinical models, as well as genomically characterized samples from clinical trials testing these drugs.

Here, by intersecting ORF resistance screening and drug combination screening data, we report that IGF1R activation confers resistance to CDK4/6 inhibitors in Ewing sarcoma. Further, the combination of CDK4/6 inhibitors and IGF1R inhibitors is synergistic in pre-clinical models of this disease, leading to enhanced cell death *in vitro* and prolongation of survival in xenograft models of Ewing sarcoma, including PDXs. IGF1R signaling has been investigated extensively in cancer, and in Ewing sarcoma, IGF1R inhibition has specifically been of interest for over a decade. The growth factor ligand of IGF1R, IGF-1, is secreted by Ewing sarcoma tumors.(49) Furthermore, a key negative regulator of IGF1R signaling, IGF binding protein 3 (IGFBP-3), is bound and inhibited directly by the EWS/FLI fusion oncoprotein, leading to constitutively active IGF1R signaling in Ewing cells.(50) In several clinical trials of IGF1R monoclonal antibodies for patients with relapsed Ewing sarcoma, there has been a durable 10–15% response rate, prompting an ongoing Phase 3 study to test IGF1R inhibitors in upfront therapy for patients with metastatic Ewing sarcoma.(51–53) Thus, combination therapies that can enhance this known, measured effect of IGF1R inhibitors are of interest, making the results of this study of particular interest to the Ewing sarcoma clinical community.

Though there has been longstanding interest in IGF1R inhibitors in Ewing sarcoma, and while IGF1R and CDK4/6 inhibitors have been studied individually in this disease,(8, 10, 11, 54) there have been no prior reports of this combination of agents in Ewing sarcoma. IGF1R and CDK4/6 dual inhibition has been studied in liposarcoma and pancreatic adenocarcinoma pre-clinical models with good effect and with minimal toxicity, similar to our findings, suggesting the potential extension of this combination to other diseases.(55, 56) In breast cancer, which is the best validated application of CDK4/6 inhibitors to date, the combination of IGF1R and CDK4/6 inhibition, with or without ER antagonists, has not yet been validated. However, with the discovery that the PI3K signaling is increased in breast cancer models after ribociclib monotherapy and is a proposed mechanism of escape, PI3K inhibitors are being tested in combination with CDK4/6 inhibitors in this disease, with clinical trials ongoing.(16, 34) Given our results that PI3K upregulation induced by ribociclib is dampened by the combination of CDK4/6 and IGF1R inhibition and that IGF1R

expression is high in a subset of patients with breast cancer,(57) an investigation of this drug combination in breast cancer would be of interest. Beyond breast cancer, there are several potential pediatric indications for testing the CDK4/6 and IGF1R drug combination. Rhabdomyosarcoma, a disease where CDK4/6 inhibitors have been effective in pre-clinical studies, has extensive pre-clinical and patient data for use of IGF1R inhibitors.(58) In neuroblastoma, another genomically quiet tumor with pre-clinical and clinical CDK4/6 inhibitor efficacy, IGF1R inhibitors have also been observed to have an effect in pre-clinical studies, as well as in a small clinical trial.(59, 60) Thus, a CDK4/6 and IGF1R inhibitor combination may be more broadly applicable in both adult and pediatric cancers.

In conclusion, we demonstrate that activation of IGF1R promotes resistance to CDK4/6 inhibitors in Ewing sarcoma and that the combination of an IGF1R with CDK4/6 inhibitor promotes a synergistic response in Ewing sarcoma cells *in vitro* and in mouse models of this disease. Based on these findings, clinical investigation of this combination of drugs for patients with Ewing sarcoma should be explored.

Supplementary Material

Refer to Web version on PubMed Central for supplementary material.

ACKNOWLEDGEMENTS

We thank the members of the RPPA core facility at MDACC for generating the RPPA data included in this manuscript. This facility is funded by NCI #CA16672. We also thank members of the Dana-Farber Cancer Institute Center for Cancer Genome Discovery (CCGD) for their assistance with the whole exome sequencing and analysis. We thank Dr. Patrick Grohar for sharing his SA-β-galactosidase staining protocol. We acknowledge Dr. Alyssa Kennedy and Dr. Akiko Shimamura for the gracious donation of the senescent mouse embryonic fibroblasts (MEFs) as well as assistance with optimizing senescence assays and the Broad Institute Cancer Cell Line Factory team for the generation of the minimally passaged Ewing sarcoma cell lines.

This work was supported by a Dana-Farber Cancer Institute/Novartis Drug Discovery Program grant (KS), the Brian MacIsaac Sarcoma Foundation (K. Stegmaier), Cookies for Kids Cancer (K. Stegmaier), the Intramural Research Program of the National Center for Advancing Translational Sciences, NIH (R. Guha, C.G. McKnight, M.I. Davis), NIH T32 CA136432–08 (L.M. Guenther, N.V. Dharia), NIH LRP L40 CA220943 (L.M. Guenther), and NIH R01 CA204915 (K. Stegmaier).

REFERENCES

1. Lawrence MS, Stojanov P, Polak P, Kryukov GV, Cibulskis K, Sivachenko A, et al. Mutational heterogeneity in cancer and the search for new cancer-associated genes. Nature. 2013;499(7457): 214–8. [PubMed: 23770567]
2. Lo-Coco F, Avvisati G, Vignetti M, Thiede C, Orlando SM, Iacobelli S, et al. Retinoic acid and arsenic trioxide for acute promyelocytic leukemia. N Engl J Med. 2013;369(2):111–21. [PubMed: 23841729]
3. Zardavas D, Baselga J, Piccart M. Emerging targeted agents in metastatic breast cancer. Nat Rev Clin Oncol. 2013;10(4):191–210. [PubMed: 23459626]
4. Hortobagyi GN, Stemmer SM, Burris HA, Yap YS, Sonke GS, Paluch-Shimon S, et al. Ribociclib as First-Line Therapy for HR-Positive, Advanced Breast Cancer. N Engl J Med. 2016;375(18):1738–48. [PubMed: 27717303]
5. Turner NC, Ro J, Andre F, Loi S, Verma S, Iwata H, et al. Palbociclib in Hormone-Receptor-Positive Advanced Breast Cancer. N Engl J Med. 2015;373(3):209–19. [PubMed: 26030518]
6. Dickson MA, Tap WD, Keohan ML, D'Angelo SP, Gounder MM, Antonescu CR, et al. Phase II trial of the CDK4 inhibitor PD0332991 in patients with advanced CDK4-amplified well-

differentiated or dedifferentiated liposarcoma. J Clin Oncol. 2013;31(16):2024–8. [PubMed: 23569312]

7. Patnaik A, Rosen LS, Tolaney SM, Tolcher AW, Goldman JW, Gandhi L, et al. Efficacy and Safety of Abemaciclib, an Inhibitor of CDK4 and CDK6, for Patients with Breast Cancer, Non-Small Cell Lung Cancer, and Other Solid Tumors. Cancer Discov. 2016;6(7):740–53. [PubMed: 27217383]
8. Kennedy AL, Vallurupalli M, Chen L, Crompton B, Cowley G, Vazquez F, et al. Functional, chemical genomic, and super-enhancer screening identify sensitivity to cyclin D1/CDK4 pathway inhibition in Ewing sarcoma. Oncotarget. 2015;6(30):30178–93. [PubMed: 26337082]
9. Esiashvili N, Goodman M, Marcus RB. Changes in Incidence and Survival of Ewing Sarcoma Patients Over the Past 3 Decades. Journal of Pediatric Hematology/Oncology. 2008;30(6):425–30. [PubMed: 18525458]
10. Perez M, Muñoz-Galván S, Jiménez-García MP, Marín JJ, Carnero A. Efficacy of CDK4 inhibition against sarcomas depends on their levels of CDK4 and p16ink4 mRNA. Oncotarget. 2015;6(38): 40557–74. [PubMed: 26528855]
11. Dowless MS, Lowery CD, Shackleford TJ, Renschler M, Stephens JR, Flack R, et al. Abemaciclib is active in preclinical models of Ewing's sarcoma via multi-pronged regulation of cell cycle, DNA methylation, and interferon pathway signaling. Clin Cancer Res 2018 8 21 [Epub ahead of print].
12. Rader J, Russell MR, Hart LS, Nakazawa MS, Belcastro LT, Martinez D, et al. Dual CDK4/CDK6 inhibition induces cell-cycle arrest and senescence in neuroblastoma. Clin Cancer Res. 2013;19(22):6173–82. [PubMed: 24045179]
13. Pikman Y, Alexe G, Roti G, Conway AS, Furman A, Lee ES, et al. Synergistic Drug Combinations with a CDK4/6 Inhibitor in T-cell Acute Lymphoblastic Leukemia. Clin Cancer Res. 2017;23(4): 1012–24. [PubMed: 28151717]
14. Geoerger B, Bourdeaut F, DuBois SG, Fischer M, Geller JI, Gottardo NG, et al. A Phase I Study of the CDK4/6 Inhibitor Ribociclib (LEE011) in Pediatric Patients with Malignant Rhabdoid Tumors, Neuroblastoma, and Other Solid Tumors. Clin Cancer Res. 2017;23(10):2433–41. [PubMed: 28432176]
15. Olanich ME, Sun W, Hewitt SM, Abdullaev Z, Pack SD, Barr FG. CDK4 Amplification Reduces Sensitivity to CDK4/6 Inhibition in Fusion-Positive Rhabdomyosarcoma. Clin Cancer Res. 2015;21(21):4947–59. [PubMed: 25810375]
16. Herrera-Abreu MT, Palafox M, Asghar U, Rivas MA, Cutts RJ, Garcia-Murillas I, et al. Early Adaptation and Acquired Resistance to CDK4/6 Inhibition in Estrogen Receptor-Positive Breast Cancer. Cancer Res. 2016;76(8):2301–13. [PubMed: 27020857]
17. Dean JL, Thangavel C, McClendon AK, Reed CA, Knudsen ES. Therapeutic CDK4/6 inhibition in breast cancer: key mechanisms of response and failure. Oncogene. 2010;29(28):4018–32. [PubMed: 20473330]
18. Condorelli R, Spring L, O'Shaughnessy J, Lacroix L, Bailleux C, Scott V, et al. Polyclonal RB1 mutations and acquired resistance to CDK 4/6 inhibitors in patients with metastatic breast cancer. Ann Oncol. 2018;29(3):640–5. [PubMed: 29236940]
19. Wang L, Wang J, Blaser BW, Duchemin AM, Kusewitt DF, Liu T, et al. Pharmacologic inhibition of CDK4/6: mechanistic evidence for selective activity or acquired resistance in acute myeloid leukemia. Blood. 2007;110(6):2075–83. [PubMed: 17537993]
20. Crompton BD, Stewart C, Taylor-Weiner A, Alexe G, Kurek KC, Calicchio ML, et al. The genomic landscape of pediatric Ewing sarcoma. Cancer Discov. 2014;4(11):1326–41. [PubMed: 25186949]
21. Sanjana NE, Shalem O, Zhang F. Improved vectors and genome-wide libraries for CRISPR screening. Nat Methods. 2014;11(8):783–4. [PubMed: 25075903]
22. Iniguez AB, Stolte B, Wang EJ, Conway AS, Alexe G, Dharia NV, et al. EWS/FLI Confers Tumor Cell Synthetic Lethality to CDK12 Inhibition in Ewing Sarcoma. Cancer Cell. 2018;33(2):202–16 e6. [PubMed: 29358035]
23. Kitchen-Goosen SM, Bowman MJ, Adams M, Berger P, Grohar PJ. The EWS/FLI1 transcriptome is characterized by marked heterogeneity across Ewing sarcoma cell lines [abstract In: Proceedings of the American Association for Cancer Research Annual Meeting 2018; 2018 4 14–18; Chicago, IL. Philadelphia (PA): AACR Abstract nr 3356.

24. Ordonez JL, Amaral AT, Carcaboso AM, Herrero-Martin D, del Carmen Garcia-Macias M, Sevillano V, et al. The PARP inhibitor olaparib enhances the sensitivity of Ewing sarcoma to trabectedin. Oncotarget. 2015;6(22):18875–90. [PubMed: 26056084]
25. Tirode F, Surdez D, Ma X, Parker M, Le Deley MC, Bahrami A, et al. Genomic landscape of Ewing sarcoma defines an aggressive subtype with co-association of STAG2 and TP53 mutations. Cancer Discov. 2014;4(11):1342–53. [PubMed: 25223734]
26. Brohl AS, Solomon DA, Chang W, Wang J, Song Y, Sindiri S, et al. The genomic landscape of the Ewing Sarcoma family of tumors reveals recurrent STAG2 mutation. PLoS Genet. 2014;10(7):e1004475. [PubMed: 25010205]
27. Cowley GS, Weir BA, Vazquez F, Tamayo P, Scott JA, Rusin S, et al. Parallel genome-scale loss of function screens in 216 cancer cell lines for the identification of context-specific genetic dependencies. Sci Data. 2014;1:140035. [PubMed: 25984343]
28. Jansen VM, Bhola NE, Bauer JA, Formisano L, Lee KM, Hutchinson KE, et al. Kinome-Wide RNA Interference Screen Reveals a Role for PDK1 in Acquired Resistance to CDK4/6 Inhibition in ER-Positive Breast Cancer. Cancer Res. 2017;77(9):2488–99. [PubMed: 28249908]
29. Yang C, Li Z, Bhatt T, Dickler M, Giri D, Scaltriti M, et al. Acquired CDK6 amplification promotes breast cancer resistance to CDK4/6 inhibitors and loss of ER signaling and dependence. Oncogene. 2017;36(16):2255–64. [PubMed: 27748766]
30. Dean JL, McClendon AK, Hickey TE, Butler LM, Tilley WD, Witkiewicz AK, et al. Therapeutic response to CDK4/6 inhibition in breast cancer defined by ex vivo analyses of human tumors. Cell Cycle. 2012;11(14):2756–61. [PubMed: 22767154]
31. Chou TC, Talalay P. Quantitative analysis of dose-effect relationships: the combined effects of multiple drugs or enzyme inhibitors. Adv Enzyme Regul. 1984;22:27–55. [PubMed: 6382953]
32. Mulvihill MJ, Cooke A, Rosenfeld-Franklin M, Buck E, Foreman K, Landfair D, et al. Discovery of OSI-906: a selective and orally efficacious dual inhibitor of the IGF-1 receptor and insulin receptor. Future Med Chem. 2009;1(6):1153–71. [PubMed: 21425998]
33. Tibes R, Qiu Y, Lu Y, Hennessy B, Andreeff M, Mills GB, et al. Reverse phase protein array: validation of a novel proteomic technology and utility for analysis of primary leukemia specimens and hematopoietic stem cells. Mol Cancer Ther. 2006;5(10):2512–21. [PubMed: 17041095]
34. Vora SR, Juric D, Kim N, Mino-Kenudson M, Huynh T, Costa C, et al. CDK 4/6 inhibitors sensitize PIK3CA mutant breast cancer to PI3K inhibitors. Cancer Cell. 2014;26(1):136–49. [PubMed: 25002028]
35. Gopalan PK, Pinder MC, Chiappori A, Ivey AM, Gordillo Villegas A, Kaye FJ. A phase II clinical trial of the CDK 4/6 inhibitor palbociclib (PD 0332991) in previously treated, advanced non-small cell lung cancer (NSCLC) patients with inactivated CDKN2A. Journal of Clinical Oncology. 2014;32(15_suppl):8077–.
36. Leonard JP, LaCasce AS, Smith MR, Noy A, Chirieac LR, Rodig SJ, et al. Selective CDK4/6 inhibition with tumor responses by PD0332991 in patients with mantle cell lymphoma. Blood. 2012;119(20):4597–607. [PubMed: 22383795]
37. Long GV, Eroglu Z, Infante J, Patel S, Daud A, Johnson DB, et al. Long-Term Outcomes in Patients With BRAF V600-Mutant Metastatic Melanoma Who Received Dabrafenib Combined With Trametinib. J Clin Oncol. 2018;36(7):667–73. [PubMed: 28991513]
38. Nazarian R, Shi H, Wang Q, Kong X, Koya RC, Lee H, et al. Melanomas acquire resistance to B-RAF(V600E) inhibition by RTK or N-RAS upregulation. Nature. 2010;468(7326):973–7. [PubMed: 21107323]
39. Solit DB, Garraway LA, Pratilas CA, Sawai A, Getz G, Basso A, et al. BRAF mutation predicts sensitivity to MEK inhibition. Nature. 2006;439(7074):358–62. [PubMed: 16273091]
40. Sherr CJ, Roberts JM. Living with or without cyclins and cyclin-dependent kinases. Genes Dev. 2004;18(22):2699–711. [PubMed: 15545627]
41. Dean JL, Thangavel C, McClendon AK, Reed CA, Knudsen ES. Therapeutic CDK4/6 inhibition in breast cancer: key mechanisms of response and failure. Oncogene. 2010;29:4018. [PubMed: 20473330]

42. McClendon AK, Dean JL, Rivadeneira DB, Yu JE, Reed CA, Gao E, et al. CDK4/6 inhibition antagonizes the cytotoxic response to anthracycline therapy. Cell Cycle. 2012;11(14):2747–55. [PubMed: 22751436]
43. Stolte B, Iniguez AB, Dharia NV, Robichaud AL, Conway AS, Morgan AM, et al. Genome-scale CRISPR-Cas9 screen identifies druggable dependencies in TP53 wild-type Ewing sarcoma. J Exp Med. 2018;215(8):2137–55. [PubMed: 30045945]
44. Sonnemann J, Palani CD, Wittig S, Becker S, Eichhorn F, Voigt A, et al. Anticancer effects of the p53 activator nutlin-3 in Ewing's sarcoma cells. Eur J Cancer. 2011;47(9):1432–41. [PubMed: 21334198]
45. Heske CM, Davis MI, Baumgart JT, Wilson K, Gormally MV, Chen L, et al. Matrix Screen Identifies Synergistic Combination of PARP Inhibitors and Nicotinamide Phosphoribosyltransferase (NAMPT) Inhibitors in Ewing Sarcoma. Clin Cancer Res. 2017;23(23): 7301–11. [PubMed: 28899971]
46. Nieto-Soler M, Morgado-Palacin I, Lafarga I, Lecona E, Murga M, Callen E, et al. Efficacy of ATR inhibitors as single agents in Ewing sarcoma. Oncotarget. 2016;7(37):58759–67. [PubMed: 27577084]
47. Grobner SN, Worst BC, Weischenfeldt J, Buchhalter I, Kleinheinz K, Rudneva VA, et al. The landscape of genomic alterations across childhood cancers. Nature. 2018;555(7696):321–7. [PubMed: 29489754]
48. Finn R, Jiang Y, Rugo H, Moulder SL, Im SA, Gelmon KA, et al. Biomarker analyses from the phase 3 PALOMA-2 trial of palbociclib (P) with letrozole (L) compared with placebo (PLB) plus L in postmenopausal women with ER + /HER2– advanced breast cancer (ABC). Annals of Oncology. 2016;27(suppl_6):LBA15.
49. Scotlandi K, Benini S, Sarti M, Serra M, Lollini PL, Maurici D, et al. Insulin-like growth factor I receptor-mediated circuit in Ewing's sarcoma/peripheral neuroectodermal tumor: a possible therapeutic target. Cancer Res. 1996;56(20):4570–4. [PubMed: 8840962]
50. Prieur A, Tirode F, Cohen P, Delattre O. EWS/FLI-1 silencing and gene profiling of Ewing cells reveal downstream oncogenic pathways and a crucial role for repression of insulin-like growth factor binding protein 3. Mol Cell Biol. 2004;24(16):7275–83. [PubMed: 15282325]
51. Pappo AS, Patel SR, Crowley J, Reinke DK, Kuenkele KP, Chawla SP, et al. R1507, a monoclonal antibody to the insulin-like growth factor 1 receptor, in patients with recurrent or refractory Ewing sarcoma family of tumors: results of a phase II Sarcoma Alliance for Research through Collaboration study. J Clin Oncol. 2011;29(34):4541–7. [PubMed: 22025149]
52. Tap WD, Demetri G, Barnette P, Desai J, Kavan P, Tozer R, et al. Phase II study of ganitumab, a fully human anti-type-1 insulin-like growth factor receptor antibody, in patients with metastatic Ewing family tumors or desmoplastic small round cell tumors. J Clin Oncol. 2012;30(15):1849–56. [PubMed: 22508822]
53. Juergens H, Daw NC, Geoerger B, Ferrari S, Villarroel M, Aerts I, et al. Preliminary efficacy of the anti-insulin-like growth factor type 1 receptor antibody figitumumab in patients with refractory Ewing sarcoma. J Clin Oncol. 2011;29(34):4534–40. [PubMed: 22025154]
54. Murakami T, Singh AS, Kiyuna T, Dry SM, Li Y, James AW, et al. Effective molecular targeting of CDK4/6 and IGF-1R in a rare FUS-ERG fusion CDKN2A-deletion doxorubicin-resistant Ewing's sarcoma patient-derived orthotopic xenograft (PDOX) nude-mouse model. Oncotarget. 2016;7(30): 47556–64. [PubMed: 27286459]
55. Miller ML, Molinelli EJ, Nair JS, Sheikh T, Samy R, Jing X, et al. Drug synergy screen and network modeling in dedifferentiated liposarcoma identifies CDK4 and IGF1R as synergistic drug targets. Sci Signal. 2013;6(294):ra85. [PubMed: 24065146]
56. Heilmann AM, Perera RM, Ecker V, Nicolay BN, Bardeesy N, Benes CH, et al. CDK4/6 and IGF1 receptor inhibitors synergize to suppress the growth of p16INK4A-deficient pancreatic cancers. Cancer Res. 2014;74(14):3947–58. [PubMed: 24986516]
57. Ochnik AM, Baxter RC. Insulin-like growth factor receptor and sphingosine kinase are prognostic and therapeutic targets in breast cancer. BMC Cancer. 2017;17(1):820. [PubMed: 29207959]
58. Pappo AS, Vassal G, Crowley JJ, Bolejack V, Hogendoorn PC, Chugh R, et al. A phase 2 trial of R1507, a monoclonal antibody to the insulin-like growth factor-1 receptor (IGF-1R), in patients

with recurrent or refractory rhabdomyosarcoma, osteosarcoma, synovial sarcoma, and other soft tissue sarcomas: results of a Sarcoma Alliance for Research Through Collaboration study. Cancer. 2014;120(16):2448–56. [PubMed: 24797726]

59. Tanno B, Mancini C, Vitali R, Mancuso M, McDowell HP, Dominici C, et al. Down-regulation of insulin-like growth factor I receptor activity by NVP-AEW541 has an antitumor effect on neuroblastoma cells in vitro and in vivo. Clin Cancer Res. 2006;12(22):6772–80. [PubMed: 17121898]
60. Geoerger B, Brasme JF, Daudigeos-Dubus E, Opolon P, Venot C, Debussche L, et al. Anti-insulin-like growth factor 1 receptor antibody EM164 (murine AVE1642) exhibits anti-tumour activity alone and in combination with temozolomide against neuroblastoma. Eur J Cancer. 2010;46(18): 3251–62. [PubMed: 20591650]

Translational Relevance:

CDK4/6 inhibitor therapy has changed treatment and outcomes for a subset of patients with breast cancer and is being investigated in multiple other malignancies. In Ewing sarcoma, CDK4 has scored as a top dependency in a genome-scale CRISPR-Cas9 screen, and CDK4/6 inhibitors are efficacious in pre-clinical models of this aggressive sarcoma. Here, we identified IGF1R activation as a mediator of resistance to CDK4/6 inhibition in Ewing sarcoma based on a genome-scale ORF resistance screen and confirmed the relevance of IGF1R activation to acquired resistance in a Ewing sarcoma cell line model. Furthermore, we established synergy between IGF1R inhibitors and CDK4/6 inhibitors *in vitro*, as well as *in vivo,* in Ewing sarcoma cell line and patient-derived xenograft (PDX) models. These findings support consideration of a clinical trial of this combination in patients with Ewing sarcoma and may have application to other pediatric and adult malignancies in which CDK4/6 inhibitors are relevant.

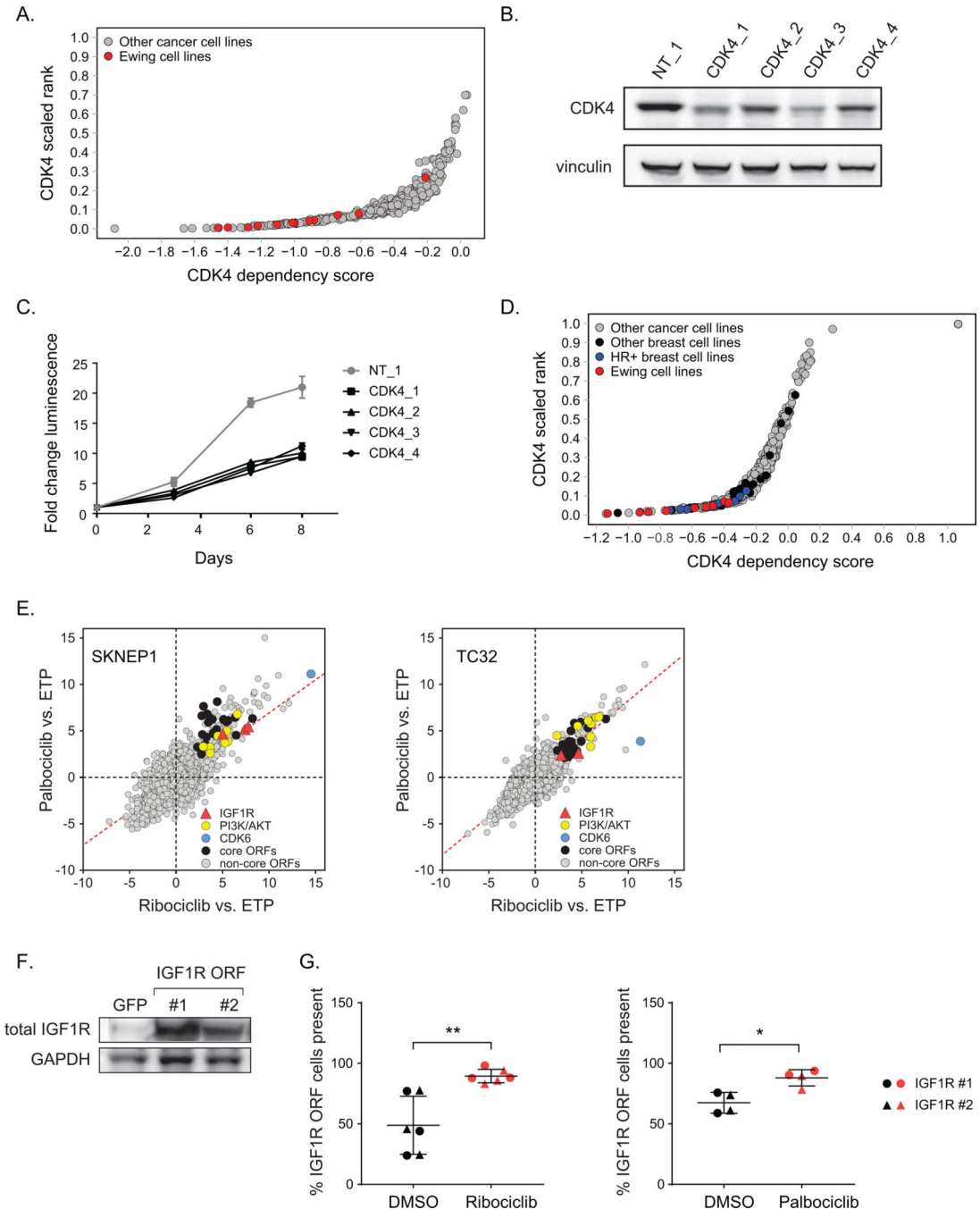

Figure 1. *CDK4* scores as a Ewing sarcoma dependency by multiple genomic screening modalities, and *IGF1R* overexpression renders resistance to CDK4/6 inhibitors in Ewing sarcoma in a genome-scale ORF screen.

Genes ranked by Ewing sarcoma-preferential dependencies in **A**. a pooled CRISPR-Cas9 screen of 476 cancer cell lines. Red circles demonstrate Ewing sarcoma cell lines. X-axis shows *CDK4* dependency score compared to other cancer cell lines screened. Y-axis shows the scaled rank of *CDK4* dependency in each cancer cell line. **B.** Western immunoblotting confirming CRISPR KO of *CDK4* in A673 cells with four unique guides, five days after puro selection. NT_1 = non-targeting control. Vinculin is used as a loading control. **C.**

Viability assay in A673 cells infected with a control (NT_1) vs. four unique *CDK4*-directed CRISPR guides. X-axis demonstrates time point of luminescence measurement, Y-axis demonstrates fold change in luminescence **D.** Scatter plot demonstrating the relative dependency of breast cancer and 9 Ewing sarcoma cell lines on *CDK4* in a pooled genome-scale shRNA screen. X-axis shows the *CDK4* dependency z-score in the indicated cell line compared to other cancer cell lines screened. Y-axis shows the *CDK4* dependency rank in each indicated cell line. Red circles represent Ewing sarcoma cell lines, blue circles represent HR+ breast cancer lines, black circles represent other breast cancer cell lines, and gray circles represent non-Ewing sarcoma, non-breast cancer cell lines. For further relevant characterization of the Ewing sarcoma cell lines included in this analysis, please see Supplemental Figure 1 and Supplemental Table 1. **E.** Scatter plots of z-scores for $\log_2$ fold changes ($\log_2$(FC)) in ORF expression for ribociclib vs. ETP (x-axis) and palbociclib vs. ETP (y-axis) in SKNEP1 (left) and TC32 (right) Ewing sarcoma cells. ORF representations for ribociclib and palbociclib treatments were significantly correlated: Pearson R = 0.68, p-value < 2.2e-16 for SKNEP1, and Pearson R = 0.81, p-value < 2.2e-16 for TC32. Genes with z-scores >2.5 with both CDK4/6 inhibitors were nominated as candidate genes conferring resistance and classified as “Core ORFs”. Two ORFs for the receptor tyrosine kinase *IGF1R* scored in both cell lines, and a third scored in SKNEP1 (red triangles). Multiple ORFs in the PI3K/AKT signaling pathway also scored (yellow circles). *CDK6* (blue circles) was included as a positive control and scored in both cell lines. See Supplemental Table 2 for full description and list of scoring “Core ORFs”. **F.** Western immunoblotting confirming overexpression of two scoring *IGF1R* ORFs in TC32 Ewing sarcoma cells compared with GFP-overexpressing ORF infected control cells (GFP) at five days post-puromycin selection. GADPH is used as a loading control. **G.** Two scoring *IGF1R* ORFs were validated in TC32 Ewing sarcoma cells by a flow cytometry-based competition assay. Cells were mixed at a 1:1 ratio with GFP-infected controls (IGF1R#1/GFP circles, IGF1R#2/GFP triangles respectively), with 50% GFP-positivity confirmed by flow cytometry on day zero and grown in continuous drug/DMSO containing media for 14 days. Dot plots demonstrate IGF1R ORF-positive cell percentage on day 14 after treatment with 1 μM of ribociclib/500 nM palbociclib (red), or equivalent DMSO control (black). Central horizontal bar represents mean, error bars represent standard deviation of 6 replicates (3 biological replicates of each *IGF1R* ORF/GFP in ribociclib/DMSO control) and 4 replicates (2 biological replicates of each *IGF1R* ORF/GFP mix in palbociclib/DMSO control), respectively. * p value < 0.05, ** p value < 0.01 by Mann-Whitney test. HR, hormone receptor.

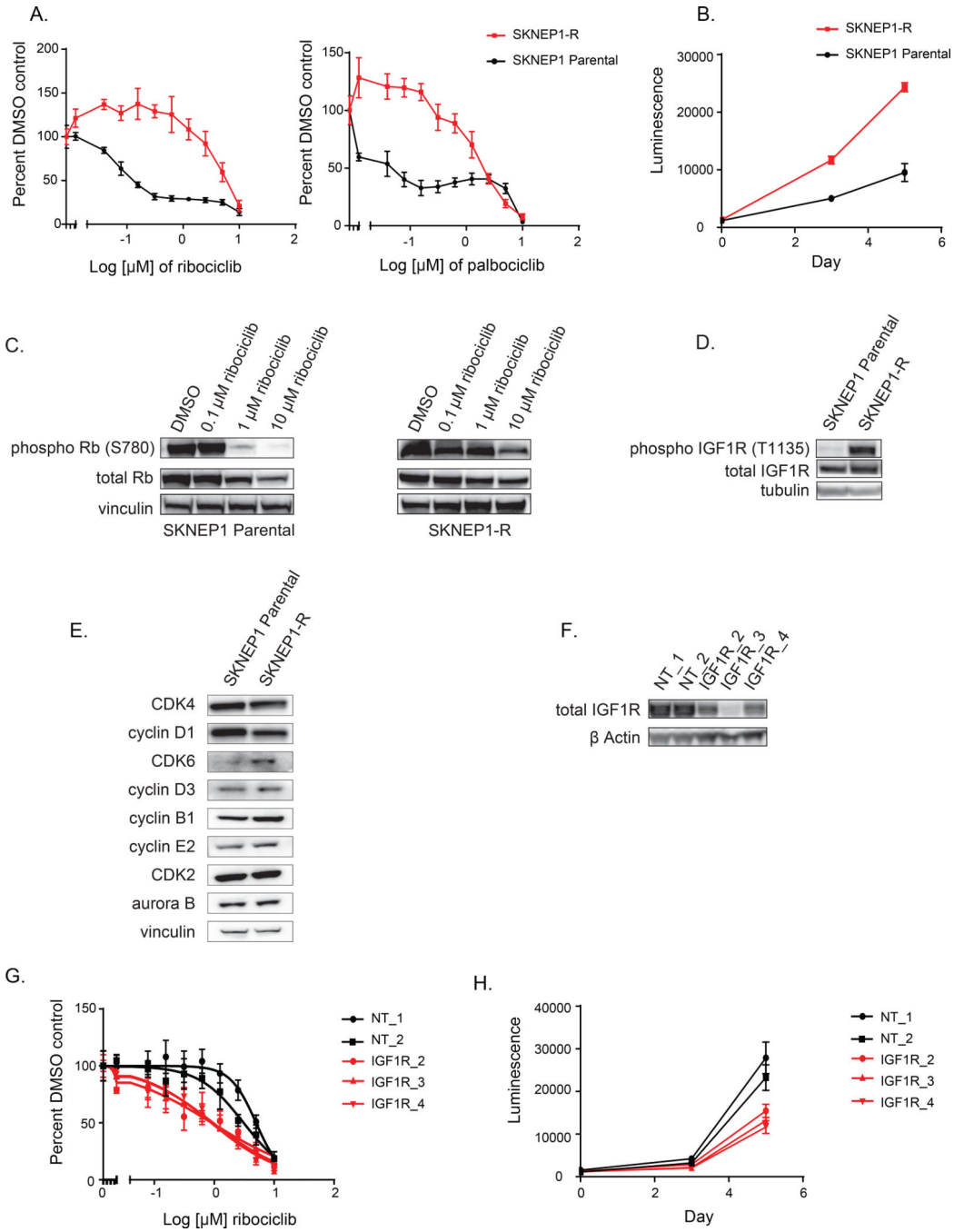

Figure 2. IGF1R activation is observed in acquired resistance to CDK4/6 inhibitors in Ewing sarcoma.

A. IC_{50} analysis of SKNEP1-R cells (red) and SKNEP1 parental cells (black) at five days after treatment with serial dilutions of 10 μM to 39 nM concentrations of ribociclib, 5 μM to 20 nM palbociclib, or relevant DMSO controls, with 4 technical replicates per treatment condition. X-axis is log[μM] of ribociclib/palbociclib, Y-axis is percent viable cells relative to the DMSO arm for each condition. Results are presented as representative dose response curves of three independent experiments. **B.** ATP-based luminescence demonstrating

differential growth of SKNEP1-R (red) cells and SKNEP1 parental cells (black). X-axis is time of luminescence read, Y-axis is raw luminescence read out. **C.** Western immunoblotting demonstrating expression of phospho and total Rb in SKNEP1-R and SKNEP1 parental cells after treatment with escalating concentrations of ribociclib for 48 hours. Vinculin was used as a loading control. **D.** Western immunoblotting demonstrating change in level of phospho-IGF1R in SKNEP1-R cells express compared to parental SKNEP1 cells. Tubulin was used as a loading control. **E.** Western immunoblotting demonstrating levels of CDK4, cyclin D1, CDK6, cyclin D3, cyclin E2, CDK2, and aurora B in SKNEP1-R cells compared with SKNEP1 cells. Vinculin was used as a loading control. **F.** Western immunoblotting confirming *IGF1R* KO in SKNEP1-R Ewing sarcoma cells after using three unique guides, six days after puro selection. NT_1, NT_2 = two distinct non-targeting guides. β actin was used as a loading control. **G.** Viability analysis of SKNEP1-R cells infected with three unique *IGF1R* CRISPR guides (red) and two NT control guides (black) at five days after treatment with serial dilutions of 10 μM to 39 nM concentrations of ribociclib or relevant DMSO control, with 4 technical replicates per treatment condition. X-axis is log[μM] of ribociclib, Y-axis is percent viable cells relative to the DMSO arm for each condition. Results are representative of two independent experiments. **H.** ATP-based luminescence demonstrating differential growth of SKNEP1-R cells infected with three unique *IGF1R* CRISPR guides (red) and two NT control guides (black). X-axis is time of luminescence reading, Y-axis is raw luminescence read out.

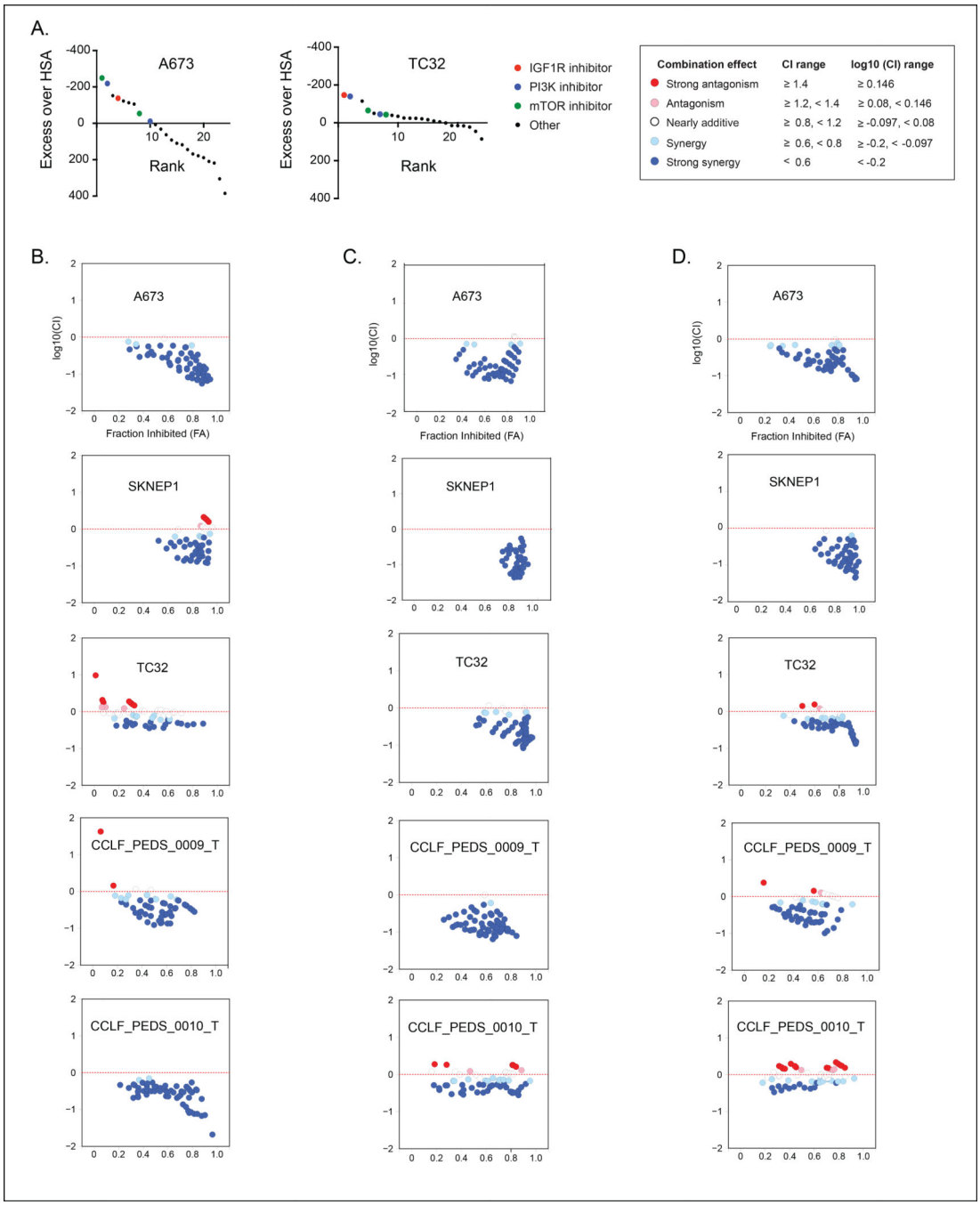

Figure 3. IGF1R inhibitors are synergistic with CDK4/6 inhibitors in Ewing sarcoma cell lines.

A. The IGF1R small molecule inhibitor BMS 754–807 (red circles) scored as synergistic with the CDK4/6 inhibitor palbociclib in a chemical screen in the Ewing sarcoma cell lines A673 (left) and TC32 (right). The screen was performed in a matrix range of 25 μM to 40 nM of each compound in five-fold dilutions with a luminescence readout after 5 days of treatment. Compounds were ranked (x-axis) by excess over highest single agent (HSA) (y-axis), with more negative as synergistic, more positive as antagonistic. Two PI3K inhibitors (blue circles) and two mTOR inhibitors (green circles) also scored in both lines. See

Supplemental Table 4 for full list of compounds screened. **B-D.** IGF1R and CDK4/6 small molecule inhibitors are synergistic across a panel of Ewing sarcoma cell lines. A673, SKNEP1, and TC32 established Ewing sarcoma cell lines and CCLF_PEDS_009_T and CCLF_PEDS_0010_T newly derived cell lines were exposed for 5 days to 20 μM down to 20 nM of each compound in two-fold serial dilutions, or DMSO control, with an ATP-based assay readout. Synergy was assessed by Chou-Talalay Combination index (CI), with x-axis representing fraction inhibited and y-axis representing $\log_{10}$(CI). CI < 0.8 is synergistic, CI ≥ 0.8 and < 1.2 is additive, and CI ≥ 1.2 is antagonistic. Combinations shown are **B.** AEW541 and ribociclib, **C.** linsitinib and ribociclib, and **D.** AEW541 and palbociclib. Classification chart for the combination index plots is included.

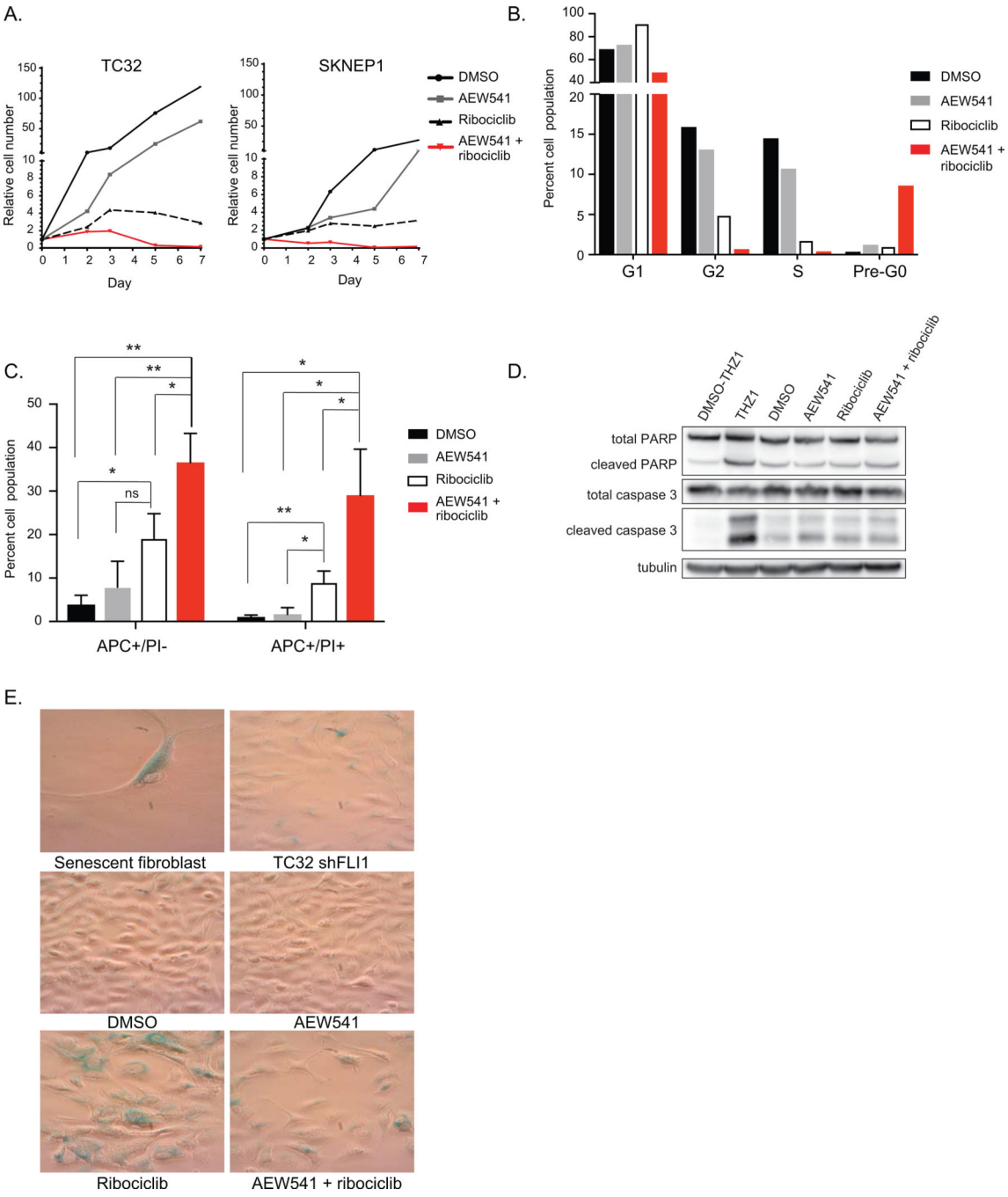

Figure 4. Ewing sarcoma cells treated with a combination of CDK4/6 inhibitor and IGF1R inhibitor exhibit a non-apoptotic cell death phenotype.

A. TC32 and SKNEP1 Ewing sarcoma cells treated with combination of AEW541 and ribociclib demonstrate cell death, with individual drug treatments causing suppressed growth. Cells were treated with 1 μM each drug or in combination, with matched DMSO control. X-axis represents time point of cell count. Y-axis is cell number relative to day zero. Results are representative of two independent experiments. **B.** TC32 cells treated for five days with 1 μM of AEW541 & 1 μM ribociclib in combination exhibit accumulation of a

pre-G0 population with propidium iodide (PI) cell cycle flow compared to matched single agent treatment or DMSO controls. Representative experiment of three independent experiments. **C.** TC32 cells similarly treated in combination as in B. demonstrated increased APC+/PI- and APC+/PI+ cells compared to either single drug treatment or DMSO, with * $p<0.05$, ** $p<0.01$ by unpaired t-tests with Benjamini, Krieger and Yakuteli two-stage step up method for controlling the False Discovery Rate. DMSO vs. AEW541 single drug treatment were not significant in either condition. **D.** Western immunoblotting demonstrating total and cleaved caspase 3 and total and cleaved PARP levels after 48 hours of drug treatment as in B. and C. TC32 cells treated for 24 hours with 80 nM of THZ1, a CDK7/12/13 inhibitor, or comparative DMSO (DMSO-THZ1), is shown as a control for cleaved PARP and cleaved caspase 3 induction. Tubulin is shown as a loading control. **E.** SA-β-gal staining of cells treated with a DMSO control, 1 μM AEW541, 1 μM ribociclib, or combination is shown compared to TC32 cells infected with a hairpin against Fli1 (shFli1) after five days of doxycycline induction and senescent mouse embryonic fibroblasts (MEFs) for positive staining controls. ns, not significant.

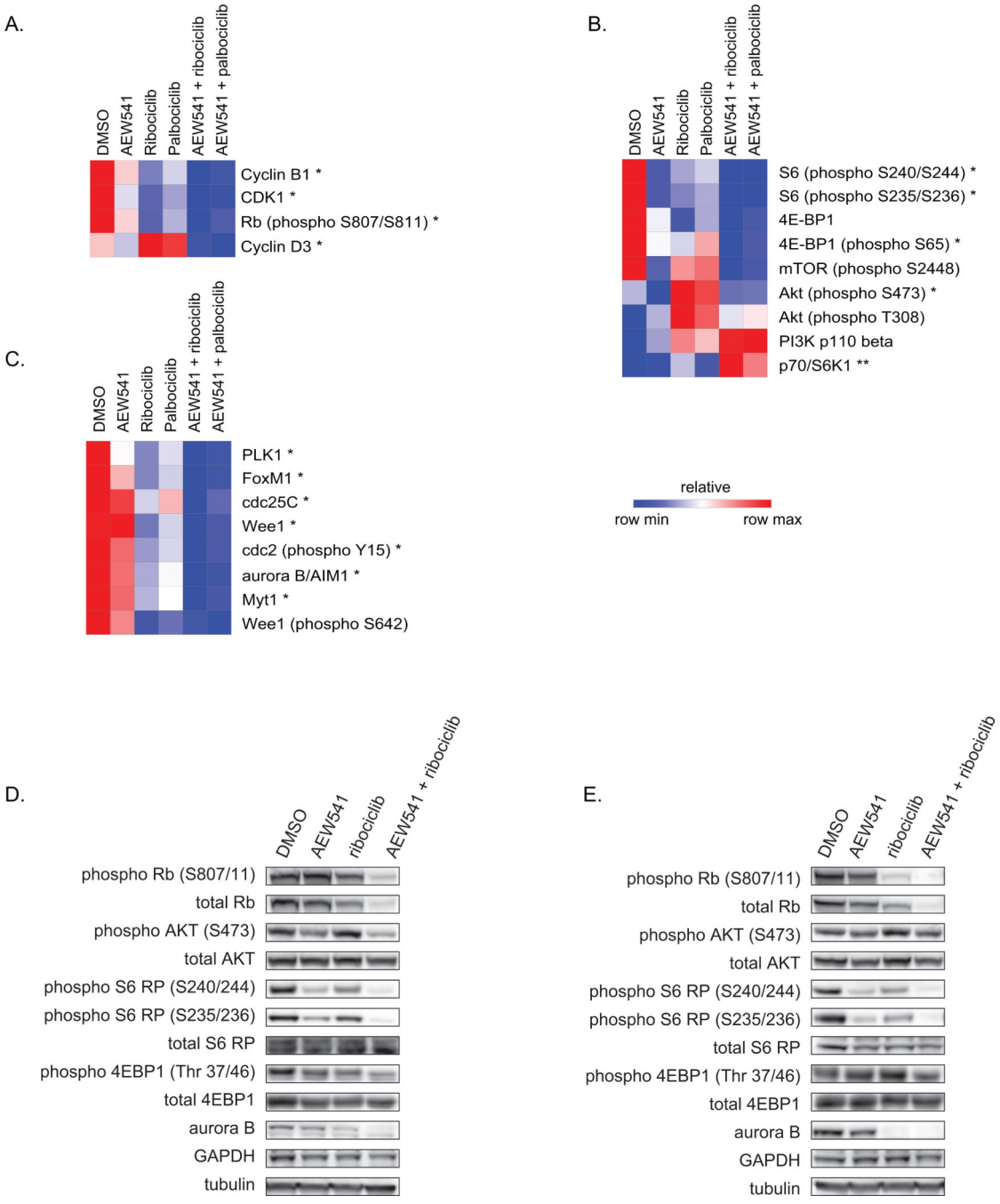

Figure 5. RPPA demonstrates enhanced effects on cell cycle proteins and PI3K/mTOR targets, as well proteins involved in mitosis, in Ewing sarcoma cells treated concurrently with ribociclib and AEW541.

TC32 Ewing sarcoma cells were subjected to RPPA analysis after 48 hours of treatment with 500 nM AEW541, 600 nM ribociclib, 100 nm palbociclib, or either combination (AEW541/ribociclib, AEW541/palbociclib), or appropriate DMSO controls, with concentrations chosen based on *in vitro* synergy analyses for lowest concentration required to achieve synergy. **A.-C.** Heat maps demonstrating a selection of the top up/down regulated proteins or phospho-proteins in the combination treated TC32 Ewing sarcoma cells, with row

normalization to a DMSO control, focusing on **A.** cell cycle proteins, **B.** PI3K/AKT/mTOR proteins, and **C.** mitosis related proteins. * indicates absolute effect size <−0.2 and ** indicates absolute effect size >0.2 of the means of combination treatment vs. means of single agents alone. **D.** Western immunoblotting validating RPPA results in select targets in the TC32 Ewing sarcoma cell line. **E.** Western immunoblotting validating RPPA results in a second Ewing sarcoma line, SKNEP1. For **D.** and **E.** GAPDH and tubulin are shown as loading controls. See also Supplemental Table 5 for a complete list of RPPA results.

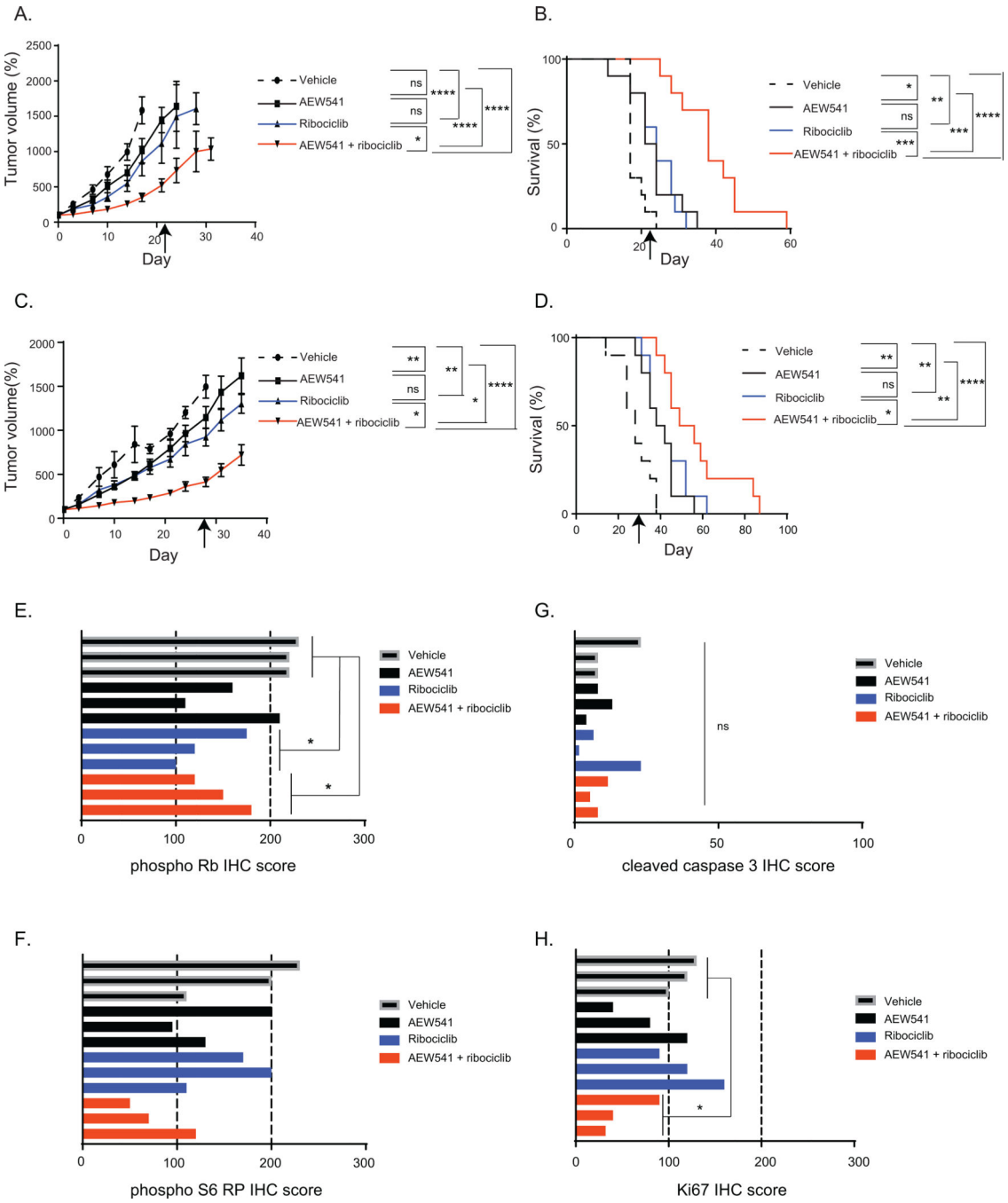

Figure 6. The IGF1R inhibitor AEW541 and the CDK4/6 inhibitor ribociclib impair tumor progression and prolong survival in two xenograft models of Ewing sarcoma.

Mice treated with a combination of AEW541 at 50 mg/kg BID and ribociclib 75 mg/kg daily for 21 days [in the A673 Ewing sarcoma cell line (**A** and **B**)] or 28 days [in PDX model (**C** and **D**)] demonstrate significantly impaired tumor growth over individual treatment arms or vehicle-treated mice (**A** and **C**). Mouse tumors were measured by calipers twice weekly. **B** and **D**, The combination demonstrates prolonged survival by Kaplan-Meier analysis. * p<0.05, ** p<0.005, *** p<0.001, **** p<0.0001 by 2-way ANOVA (A and C) and log-

rank test (B and D). (ns = not significant). Arrow indicates end of drug/vehicle treatment. Bar graphs demonstrating IHC quantification of **E.** phospho Rb (pRb) staining, **F.** phospho S6 kinase (pS6K) staining, **G.** cleaved caspase 3 staining, and **H.** Ki67 staining in three mice per treatment group in the PDX model after five days of treatment. * $p<0.05$ by Student's T-test, other combinations not marked were non-significant by Student's T-test. See also Supplemental Figure 4 and 5.